Supplementary Information for

"One-to-three" droplet generation in digital microfluidics for parallel on-chip chemiluminescence immunoassays

Kai Jin,[ab] Chenxuan Hu,[b] Siyi Hu,[b] Chengyou Hu,[c] Jinhua Li,*[a] Hanbin Ma*[b]

a. Ministry of Education Key Laboratory for Cross-Scale Micro and Nano Manufacturing, Nanophotonics and Biophotonics Key Laboratory of Jilin Province, School of Science, Changchun University of Science and Technology, Changchun, Jilin province, 130022, P.R.China.

b. CAS Key Laboratory of Bio-medical Diagnostics, Suzhou Institute of Biomedical Engineering and Technology, Chinese Academy of Sciences, No.88 Keling Road, Suzhou, Jiangsu province, 215163, P.R. China

c. Guangdong ACXEL Micro & Nano Tech Co., Ltd, China

* Corresponding author: mahb@sibet.ac.cn (H. Ma); lijh@cust.edu.cn (J. Li).

Appendix Ⅰ. Theoretical analysis of droplet splitting

For conventional droplet splitting shown in Fig. 1(b), according to Laplace Equation, the droplet pressure P can be expressed by the radius of curvature as:

$$P_2 - P_a = \gamma(\frac{1}{r2} + \frac{1}{R2}) \tag{8}$$

$$P_1 - P_a = \gamma(\frac{1}{r1} + \frac{1}{R1}) \tag{9}$$

$$P_c - P_a = \gamma(\frac{1}{rc} + \frac{1}{Rc}) \tag{10}$$

Here, P_a represents the atmosphere pressure. the pressure difference between droplets P_2 and P_c, and P_2 and P_1 can be obtained by simultaneous Equations (8) (9) (10) with (1) (2):

$$\Delta P_{2c} = P_2 - P_c = \gamma\left[\frac{1}{R_2} - \frac{1}{R_c} + \frac{\cos\theta_{Vc} - \cos\theta_{V2}}{d}\right] \tag{11}$$

$$\Delta P_{21} = P_2 - P_1 = \gamma\left[\frac{1}{R_2} - \frac{1}{R_1} + \frac{\cos\theta_{V1} - \cos\theta_{V2}}{d}\right] \tag{12}$$

Here, θ_{vc}, θ_{v2}, and θ_{v1} respectively represent the contact angles of the droplet at different positions and at the bottom plate when the droplet is split, where θ_{v2} and θ_0 are equal. When a sufficiently high voltage is applied, the droplet contact angle θ_{vc} reaches a value where the droplet is split. It can be seen from Fig. 1(b) that R_c remains basically unchanged during the splitting process. As the radius of the splitting site R_2 decreases, ΔP_{2c} also gradually decreases. When ΔP_{2c} tends to zero, the splitting ends with child droplets generation [18]. At this time, the minimum value of the radius of curvature, R_2 is close to half of the square electrode side length, while R_c is half of the electrode side length as well, that is $|R_2|_{min} = R_c$ ($-R_2 = R_c$) [9]. Due to the contact angle saturation of the EWOD actuation, there is an upper limitation of the EWOD forces. If the channel gap d increases, the term $\frac{\cos\theta_{Vc} - \cos\theta_{V2}}{d}$ of Equation (11) decreases, and the EWOD actuation may not be sufficient enough to overcome the capillary forces impeding movement [24]. So channel gap d of Fig.1(b) for sufficient droplet movement has a maximum value：

$$d_{max} = \frac{R_c}{2}\left(\cos\theta_{Vc} - \cos\theta_0\right) \tag{13}$$

As shown in Fig. 1(c), the key of the “one-to-three” droplet splitting method to obtain sub-droplets is to retain the droplet at the neck position when the two mother droplets split. Here we extend the theoretical analysis of $P_2 - P_c = 0$ into the unidirectional droplet splitting of Fig. 1(b). As

indicated by Cho et. al. [9], in static equilibrium, the pressure should be equal inside the droplet. For the "One-to-three" droplet splitting, ideally R_2 is equal to $R_{2'}$, P_2 is equal to $P_{2'}$, Thus:

$$2P_2 - P_c^{'} = \gamma\left[\left(\frac{2}{r_2} - \frac{2}{R_2}\right) - \left(\frac{1}{r_c{}'} - \frac{1}{R_c{}'}\right)\right] = 0 \tag{14}$$

Solve Equation (14) with (1) and (2):

$$2P_2 - P_c^{'} = \gamma\left[\left(\frac{2}{R_2} - \frac{1}{R_c}\right) + \frac{\cos\theta_{Vc} - 2\cos\theta_0 - \cos\theta_t}{d}\right] = 0 \tag{15}$$

The channel gap of Fig.1(c) is related to contact angle difference and radii of curvature by simplification:

$$d_{max} = \frac{R_c}{3}\ (\cos\theta_{Vc} - 2\cos\theta_0 - \cos\theta_t) \tag{16}$$

Then, Equation (16) is subtracted from Equation (13)：

$$\Delta d_{max} = \frac{R_c}{3}\ (\cos\theta_{Vc} + \cos\theta_0 + 2\cos\theta_t)\ < 0 \tag{17}$$

In summary, the “one-to-three” droplet splitting method improves the maximum gap of droplet splitting to a certain extent.

Appendix Ⅱ. DMF parallel chemiluminescence immunoassay platform and DMF Chip

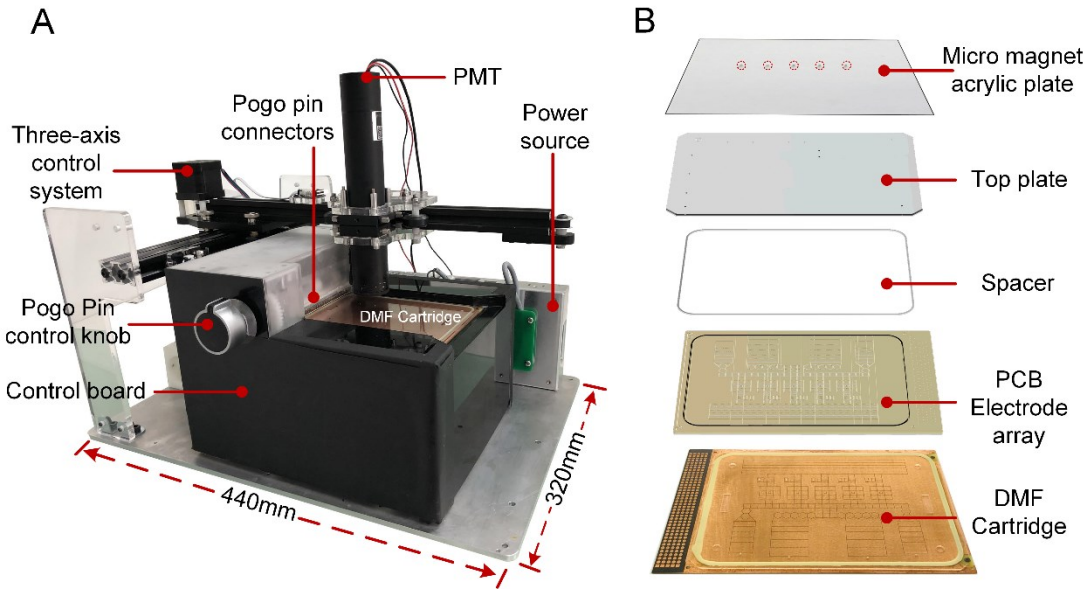

Fig. S1 A. The Photograph of DMF Chemiluminescence immunoassay platform, including photomultiplier tube (PMT), three-axis control system, power supply, Pogo Pin control knob, Pogo Pin connectors. All components are fixed on a 440mm*320mm steel plate. B. Exploded view of DMF cartridge for CLIA.

Appendix Ⅲ. Linear fitting curve of different concentrations of (HRP)

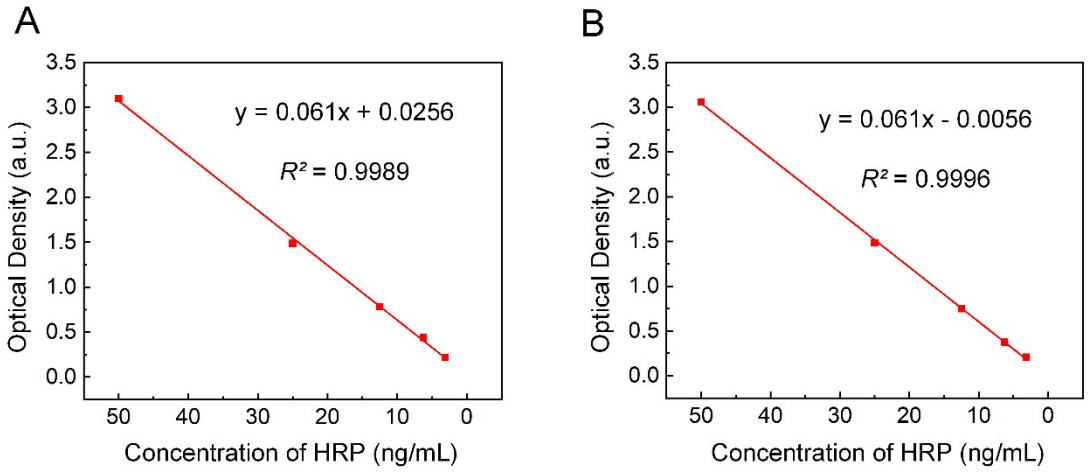

Fig. S2 A. Absorbance test carried out on a microplate reader after the HRP standard solution reacts with TMB. B. Absorbance test after the HRP standard solution containing surfactant 90R4 reacts with TMB.

Appendix Ⅳ. Comparison of uniformity of droplets generated with different methods.

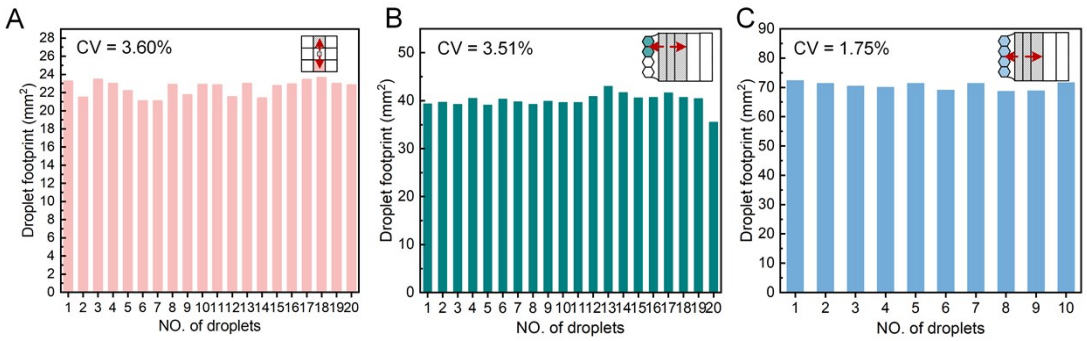

Fig. S3 A. Footprints of bottom mother droplet by "one-to-three" methods. B, C. The droplet footprints area of two droplets and four droplets generated by hexagonal electrode from reservoir.

Appendix Ⅴ. Contact angles change with respect to applied voltages on different surfaces.

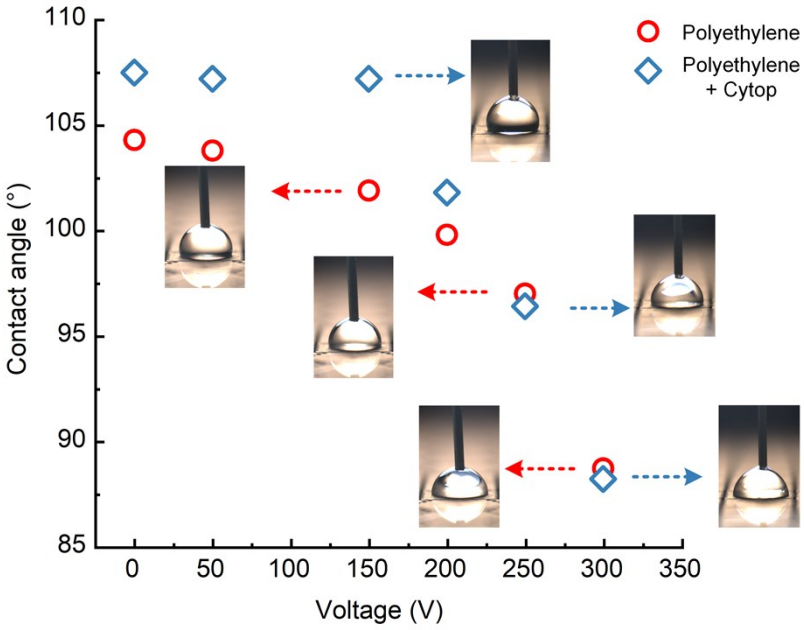

Fig. S4 Drop a droplet of 10uL volume on the surface of the PE film and PE film coated with Cytop respectively, then measure the contact angle changing with applied voltages.

Although the initial contact Angle of PE film coated with CYTOP is larger than that of PE film, the contact angles under working voltage are similar, so we consider they have the same ability to drive droplet.

Appendix Ⅵ. Comparison of the experimental value and theoretical value of magnetic beads washing efficiency

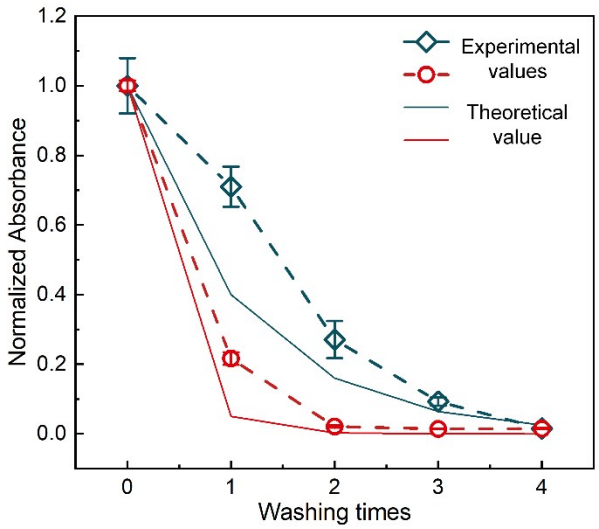

Fig. S5 Experimental value: The washing efficiency of method 1 and method 2 is compared by measuring the enzyme concentration in the waste liquid after washing. Error bars represent the standard deviation of three replicate experiments. Theoretical value: the estimated value based on the proportion of the remaining liquid volume in each wash to the total liquid volume.

The above figure is an extension of Fig. 5 (b) of the main text, and the experimental values are consistent with it. Obviously, the washing efficiency of the theoretical value is higher than that of the experimental value. The possible reason is: (1) 1/20 and 2/5 are estimated values, deviated from actual volume of splitted droplet. (2) Binding efficiency of protein to magnetic beads is uncertain in magnetic bead solution containing free HRP.

Appendix Ⅶ. Comparison with more washing strategies

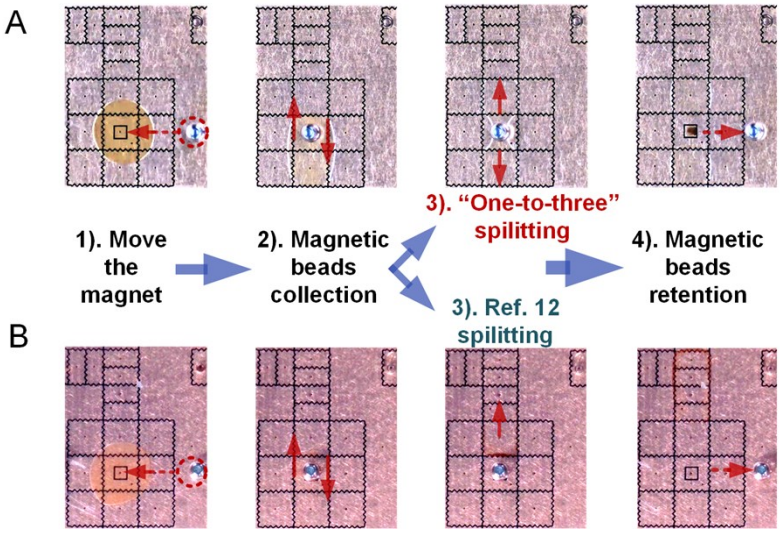

Fig. S6 A. Magnetic bead washing method strategies on "one-to-three" droplet splitting method. B. Magnetic bead washing method according to references 12.